RESEARCH ARTICLE OPEN ACCESS

Greener cum chemical synthesis and characterization of Mg doped ZnS nanoparticles and their engineering band gap performance

Joy Prabu. H*, Johnson. I
Department of Physics, Centre for Nano sciences and Applied Thermodynamics, St. Joseph's College (Autonomous), Trichy-620 002

GRAPHICAL ABSTRACT

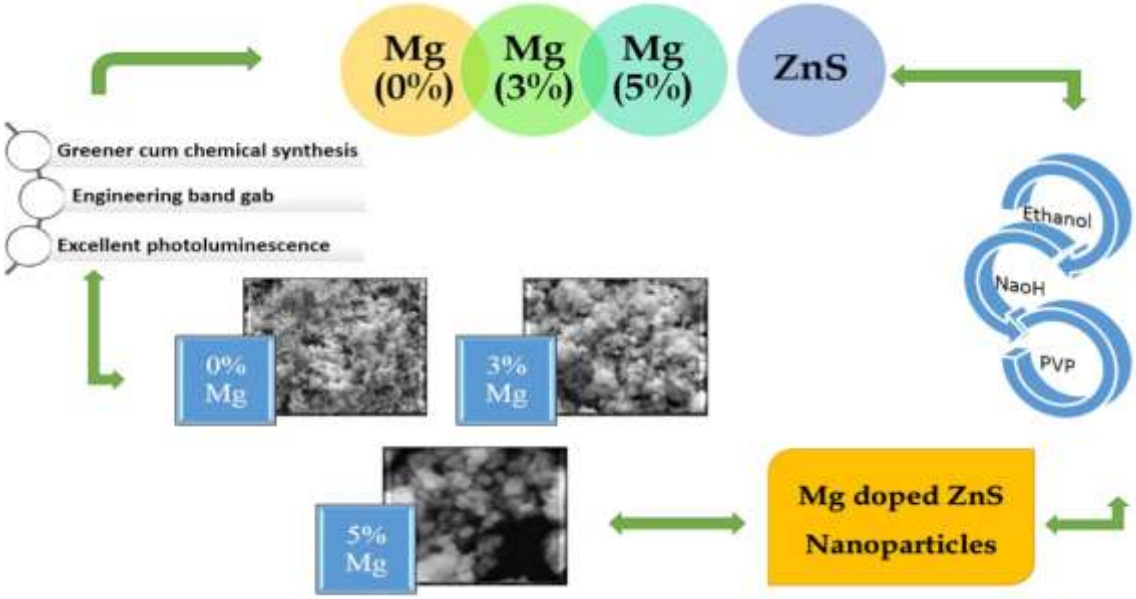

ABSTRACT
In the present investigations, high-quality Mg doped ZnS nanoparticles were synthesized by Greener cum chemical process with the assistance of polyvinyl pyrrolidone (PVP) with two different Mg concentrations. Doping of Mg metal in nanoparticles were found to be a good technique for tuning the band gap of ZnS nanoparticles. Simultaneously, Mg doping also inhibited the growth of particle size and it decreased from 33.2 nm to 18.3 nm with the increase in doping concentration from 0% to 5%. Band gap was found to rise from 3.12 eV to 3.38 eV and photoluminescence studies exposed that visible Photoluminescence (PL) emission was improved with doping concentration. The nanoparticles have been characterized by Field Emission Scanning Electron Microscopy (FESEM), X-Ray Diffraction (XRD), Fourier Transform Infrared (FTIR) spectroscopy, Ultra Violet visible (UV–vis) spectroscopy, and Energy Dispersive X-ray Analysis (EDAX).

Keywords **-** Band gap, Greener cum chemical technique, Honeycomb structure, X-ray diffraction, ZnS

I. INTRODUCTION

Nanostructure materials draw the attention of scientific world due to their various potential applications in the fabrication of optoelectronic and micro-electronic devices [1]. The explosion in both academic and industrial interest over the past twenty years arises from the remarkable variations in fundamental electrical, optical and magnetic properties that occur as one progress from an "infinitely extended" solid to a particle of material consisting of a countable number of atoms. Among various classes of nanoparticles, II-VI class inorganic semiconductor nanomaterials [2] like CdSe, CdS, and ZnS [3] emerged as significant materials for the applications in optoelectronic devices. ZnS is extensively studied as it has plentiful applications to its credit.

Nano structured ZnS such as nanocrystals, nanowires, and nano belts exhibit excellent optical and electronic performances, which differ much from bulk ZnS material due to three-dimensional electrons and holes confinement in a small volume. The surface of a nano particle is more important than bulk

because nano particles have larger surface to volume ratios. Surface atoms are bound by weaker forces because of missing neighbors, which lead to high surface reactivity.

To date, there are many methodologies available for synthesizing ZnS nanoparticles, such as laser ablation, electrochemical fabrication, Solvo-thermal and sol-gel methods. However, Greener cum chemical technique is one of the more extensively renowned approaches due to its multiple advantages, for instance, environmentally benign, easy to handle, and requiring no costly equipment. Doping with suitable elements is an effective method to adapt and control the optical properties of ZnS nanoparticles, which is decisive for its real-world applications [4].

Luminescence measurements were recognized as one of the most significant techniques to reveal the energy structure and surface states of these particles. Localized trap states were studied in detail inside the band gap to recognize the sub-band gap energy levels. It was found that the defect levels play a vital role in determining the luminescence characteristics of the Mg doped ZnS nanoparticles. This doping reasons a visible orange luminescence at about 585 nm. It is well known that ZnS doped with Mg shows attractive light-emitting properties with increased optically active sites for applications as efficient phosphors [5,6].

In this work, we have mainly focused on preparing and investigating toxicity free Mg doped ZnS nanoparticles with varying Mg concentrations in the presence of polyvinylpyrrolidone (PVP). This has afforded a facile method permitting its use as a common diagnosis reagent. To this end, the nanoparticles should be made with a dimension of 18-33 Å and be stable (aggregation prevention). Keeping in view of the obvious advantages of this technique, we have made an attempt to synthesize Mg doped ZnS nanoparticles and the experimental results are presented in this paper.

II. MATERIALS AND METHODS

2.1 Materials

All reagents were purchased in analytical grade (Sigma Aldrich, Germany) and used without further purification. Mg doped ZnS nanoparticles were prepared using zinc acetate dihydrate and magnesium chloride hexahydrate in the presence of polyvinylpyrrolidone (PVP) (MW ~55,000). Hydrochloric acid and sodium hydroxide were used to maintain pH variations of sample solutions. Double-distilled water was used as a solvent.

2.2 Preparation of Mg doped ZnS nanoparticles

Mg doped ZnS nanoparticles were synthesized based on the reaction of the mixture of zinc acetate dihydrate [Zn $(CH_3COO)_2$. $2H_2O$] and magnesium chloride hexahydrate [$MgCl_2$. $6H_2O$] with 1465 mg PVP (Sigma Aldrich, MW ~55,000) in aqueous media.

In a typical synthesis process, Mg doped ZnS nanoparticles were prepared using zinc acetate and magnesium chloride. A highly pure ZnS powder (99.9%) of 4.87 g was taken and 50 ml of ethanol was added [7]. The mixture was stirred and heated until a clear homogeneous solution is obtained. Then, the solution was allowed to cool to attain the room temperature (28°C). When the solution reached the room temperature, 3 M of NaOH (Merck) was made by dissolving the PVP, and it was added to it and stirred for 30 minutes [8,9].

Afterwards, the doping material $MgCl_2$ (concentrations of Mg in 0%, 3% and 5%) was taken and 50 ml of distilled water was added drop by drop under magnetic stirring. The resultant solution was centrifuged at 3000 rpm for 10 minutes. The centrifuged supernatant liquid was collected and then centrifuged twice at 15000 rpm for 30 minutes. The suspended pellet was purified with ethanol and agitated for 2 minutes using ultrasonic bath. This procedure resulted in the formation of a semi liquid nanoparticles which were washed with water and ethanol several times to remove by-products and then dried at 100°C for 12 hours in a hot air oven. The purified pellets were then dried and the powder was obtained. This was used for further characterization. At the end, the dried powder was further calcined at 300°C for 5 hours which resulted in the formation of Mg doped ZnS NPs.

2.3 Characterization techniques

The crystallanity, structure and crystallite size of Mg-doped ZnS NPs were determined by X-ray diffraction (XRD) pattern using PAN alytical X'pert MPDPRO with Cu Kα radiation (1.5405 Å) source (45kV, 35 mA). The morphology of the products was investigated by field-emission scanning electron microscope (FESEM) using JEOL (JSM-7000F) at an accelerating voltage of 20 kV. The compositional analysis was carried out using EDAX attached with the FESEM. UV–visible absorbance spectra were recorded using Perkin Elmer Lambda 35 UV/vis spectrometer. FTIR spectra of as-prepared samples were recorded using a Fourier transform infrared spectrometer (Spectrum 65, PerkinElmer) in the range of 4000–400 cm^{-1} with a resolution of 1 cm^{-1}. The PL measurements were carried out using a luminescence spectrometer (LS-55B, PerkinElmer) with a Xenon lamp as the excitation source. The excitation wavelength used for the experiment was 573 nm.

III. RESULTS AND DISCUSSION

3.1 Powder X-ray diffraction

The characteristic XRD spectra of the pure ZnS and Mg-doped ZnS NPs are shown in Fig. 1. The

peak positions of each sample reveal the hexagonal wurtzite structure of ZnS which were confirmed from the standard JCPDS card no. 36-1450. Further, there is no other peak was observed in the XRD patterns. Which revealed the purity of the nanoparticles [10,11].

Debye- Scherrer's formula was used to calculate crystallite size:

$$D = \frac{0.9\lambda}{\beta cos\theta}$$

Where λ is the wavelength of X-rays, β is the full width at half maximum (FWHM) of the peaks at the diffracting angle θ.

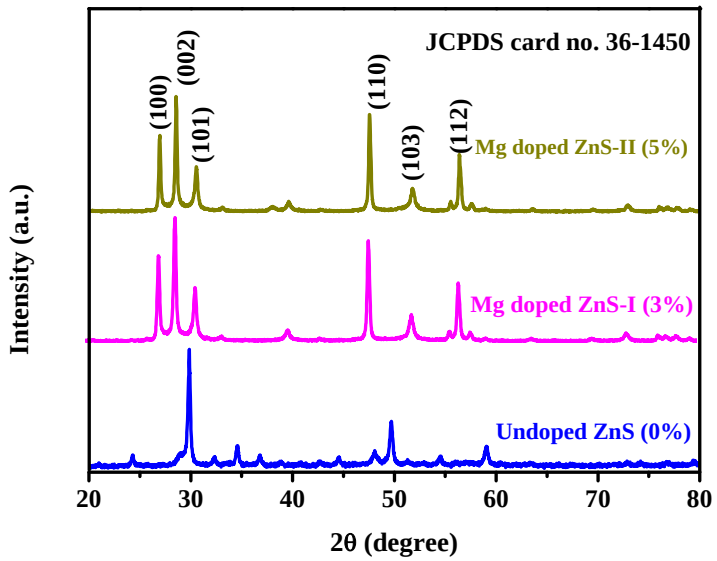

Fig. 1. X-ray diffraction patterns of pure ZnS, 3% & 5% Mg doped ZnS.

In addition, we did not observe any diffracted peaks due to Mg in the XRD pattern because of very low concentration of the Mg in the nanoparticles. On the basis of the full width at half-maximum of peak and applying the Debye– Scherrer equation, the calculated average crystallite size of different samples are listed in Table 1.

It can be observed that the crystallite size of ZnS decreases from 33.2 nm to 18.3 nm when Mg content increases from 0% to 5%. The data reveals that the presence of Mg ions in ZnS prevents the growth of crystal grains [12].

Table 1 Crystallite size of different samples

S. No	Mg concentration (%)	Crystallite size (nm)
1	0	33.2
2	3	20.4
3	5	18.3

3.2 Morphological and compositional analysis by field-emission scanning electron microscope (FESEM) and EDAX

The FESEM images clearly show that Mg doped ZnS nanoparticles become more uniform than undoped ones, and the sizes of the prepared ZnS samples have not been significantly altered due to the incorporation of Mg atoms. From the overall morphology of Mg doped ZnS (Fig. 2), we can indicate that the sample is composed of numerous nearly-monodispersed honeycomb structure with hollow nanospheres formed [13-16]. This indicates that the walls of the hollow nanospheres have a relatively high compactness and stability. The average particle size (around 20 nm- 35 nm) and further observation shows that the sphere consists of numerous tiny particles with the size of tens of nanometers. The shape of a, b & c samples have no major difference.

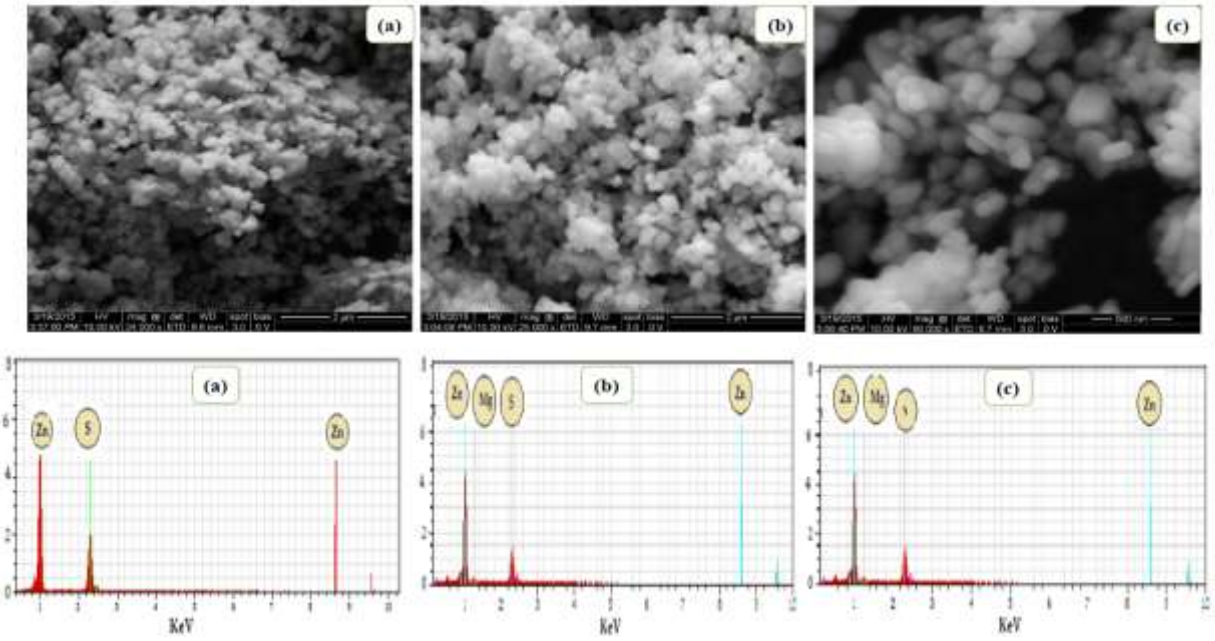

Fig. 2. FESEM and EDAX images of (a) Undoped ZnS (b) 3% Mg doped ZnS and (c) 5% Mg doped ZnS nanoparticles.

The nanoparticles were subjected to EDAX analysis (Fig. 2) which shows the general composition of the studied Mg and ZnS confirming the presence of Mg, Zn and S. The detailed elemental compositions are presented in Table 2.

Table 2 Elemental composition of undoped and Mg doped ZnS NPs.

S. No.	Sample	Elements	Atomic (%)	Weight (%)
1	Undoped ZnS	Zn S	72.35 27.65	56.20 43.80
2	(3%) Mg doped ZnS	Zn S Mg	66.95 30.53 2.52	49.23 45.78 4.99
3	(5%) Mg doped ZnS	Zn S Mg	65.44 29.85 4.71	48.21 45.77 6.02

3.3 Fourier transform infrared spectroscopy (FTIR)

To further ascertain, the surface properties of Mg doped ZnS nanoparticles, the FTIR spectrum was recorded and shown in Fig. 3. The obtained peak values are in good agreement with the reported values. It can be seen from (Fig. 3) that there are clear variations in the positions and sizes of FTIR peaks representing, that Mg might have been incorporated in ZnS host [17,18].

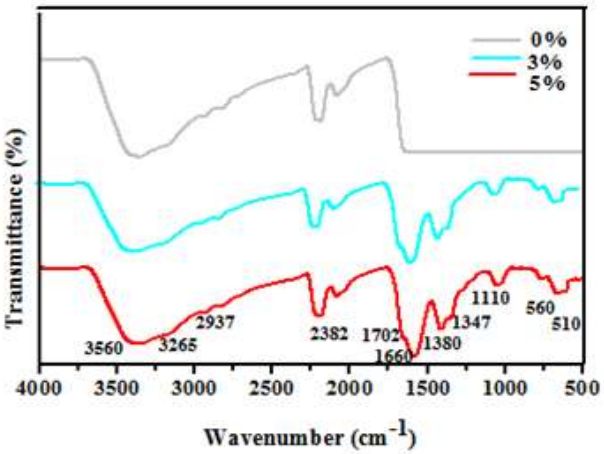

Fig. 3. FTIR spectra of different compositions of pure and Mg doped ZnS NPs.

In the PVP capped Mg doped ZnS nanoparticles, the absorption peaks at 2937 cm^{-1} correspond to -C=O stretching, 1007 cm^{-1} is attributed to -C=N stretching. The formation of co-ordinate bond between the nitrogen atom of the PVP and the Zn^{+2} ions is believed to be present. A wide band in the region of 3560–3265 cm^{-1} has been assigned to the stretching vibration mode of a hydroxyl group [19].

In plots for Mg doped ZnS, wide bands at 1347cm^{-1} are attributed to the Mg-O stretching vibration while it is entirely absent in the undoped ZnS sample. By reason of the high surface-to-volume ratio as well as the complex surface conditions, the Mg doped ZnS nanoparticles possibly have more defect states than bulk materials, which may be the reason for having certain novel properties.

Assignments of IR band frequencies of vibrational frequencies have been provided in Table 3.

Table 3 Assignments of IR band frequencies (cm^{-1}) of pure and Mg doped ZnS

Vibrational assignment	Vibrational frequencies
O–H stretching	3560-3265
-C=O stretching	2382-2937
O–H stretching	1660-1380
C-O stretching	1110
-C=N stretching	1702
Zn-S stretching	510-560
Mg–O stretching	1347-1380

3.4 Optical properties

The optical absorption of the undoped and different concentrations of Mg doped ZnS nanoparticles have been analyzed in de-ionized water as shown in Fig. 5. In order to determine the optical band gaps and associated properties, the optical absorbance measurements were carried out at room temperature and the absorbance spectra of undoped and Mg doped ZnS NPs are shown in Fig. 4. Since doped nanostructures are expected to have different optical properties compared to undoped nanostructures [20].

Absorbance spectra exhibit an absorption peak around 460 nm for pure ZnO. There is a clear blue shift with Mg doping and absorption peak for 5% Mg doped ZnO shifted to 427 nm, which can be attributed to the quantum confinement effect.

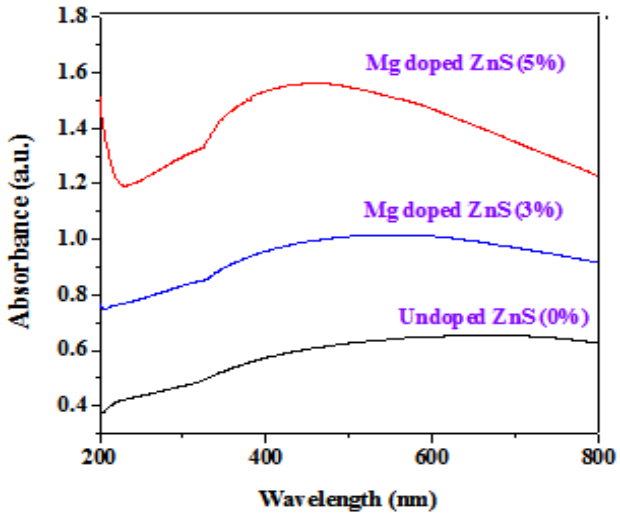

Fig. 4. Absorbance spectra of undoped ZnS and Mg doped ZnS samples.

Optical band gap for all samples was calculated using well known Tauc relation given by:

$$Ah\upsilon = A'(h\upsilon - Eg)^n$$

where $\alpha = 2.303\ A/t$ is called the absorption coefficient, A is the absorbance, t is the path length of wave which is equal to the thickness of the cuvette, A′ is the proportionality constant, Eg is the band gap, hυ is the photon energy and n =1/2 and 2 for direct and indirect band gap semiconductors respectively. It can be seen from Tauc plots as shown in Fig. 5, that the band gap of the prepared nanoparticles is 3.12, 3.26 and 3.38 eV respectively. On doping with Mg, the particle size decreases as a result of which band gap increases [21].

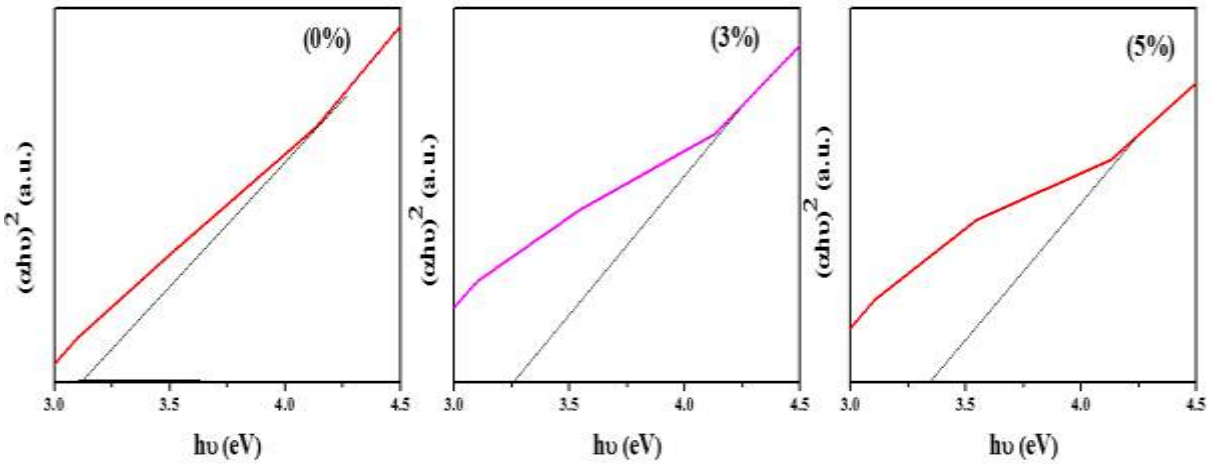

Fig. 5. Tauc plots of pure and Mg doped ZnS nanoparticles.

3.5 Photoluminescence

PL spectrum is an effective way to study the electronic structure, optical and photochemical properties of semiconductor materials, by which information such as surface oxygen vacancies and defect, the efficiency of charge carrier trapping, immigration and transfer can be obtained.

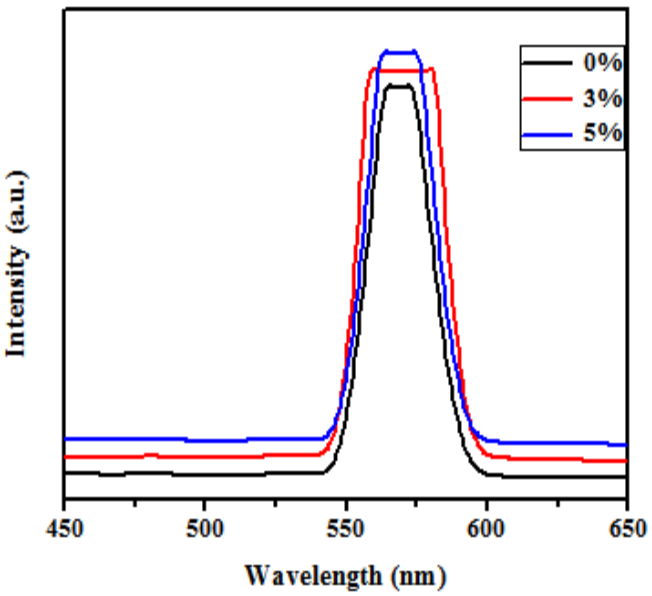

Fig. 6. Photoluminescence spectra of pure and Mg doped ZnS NPs.

Photoluminescence property of the samples was investigated at room temperature. For Mg doped ZnS nanoparticles, two different emission bands are existing in the fluorescence spectra: the first emission band, at around 480 nm, also existed in the emission spectrum of the undoped ZnS nanoparticles. This emission band is due to the host ZnS but not from Mg ions. Upon Mg doping, a second typical emission band centered around 574 nm is developed for the well-known based orange emission while ZnS with surface bound Mg^{+2} yielded the ultraviolet emission. Thus, it could be determined that the Mg^{+2} ions in our samples were incorporated into the host ZnS nanoparticles.

Hence, it is clear from Fig. 6 that the intensity of broad deep level emission increases considerably with the increase in Mg doping concentration. The incorporation of Mg^{+2} in ZnS lattice may be the reason for the formation of different intrinsic defects which lead to the enhanced visible emission.

IV. CONCLUSION

Mg doped ZnS nanoparticles with very narrow size distribution were prepared from Greener cum chemical technique in aqueous medium at air atmosphere were systematically investigated. The structure, optical properties, band gap, morphology and composition of the samples were determined by XRD, FTIR, UV-VIS, FESEM and EDAX spectra analyses. The XRD patterns exhibit the wurtzite structure of all the samples and no impurity phase was observed. It was found that as Mg concentration increases there is a decrease in crystallite size (33.2 nm to 18.3 nm) and lattice constant. FESEM shows the particle sizes ranging from 20 nm to 35 nm and honeycomb structure with hollow nanospheres. PL spectrum indicates that ultraviolet emission peak blue shifts from 573 nm to 428 nm as the Mg content increased from 0 % to 5%, which coincides with the results from the absorption spectrum. It is observed that the ZnS band gap, with the range of 3.12 eV to 3.38 eV, can be controlled only by changing Mg contents. The Photoluminescence study shows an increase in the visible emission with the increase in doping concentration. In conclusion, Mg doping in ZnS is an effective method to improve its optical properties like luminescence and band gap, which makes it a noble material for optoelectronic applications.

REFERENCES

[1] Y. Wang, X. Zhao, L. Duan, F. Wang, H. Niu, W. Guo and A. Ali, Structure, luminescence and photocatalytic activity of Mg-doped ZnO nanoparticles prepared by auto combustion method, Materials Science in Semiconductor Processing, 29, 2015, 372-379.

[2] S. Hajati, M. Ghaedi, F. Karimi, B. Barazesh, R. Sahraei and A. Daneshfar, Competitive adsorption of Direct Yellow 12 and Reactive Orange 12 on ZnS: Mn nanoparticles loaded on activated carbon as novel adsorbent, Journal of Industrial and Engineering Chemistry, 20, 2014, 564-571.

[3] F. Chen, Y. Cao and D. Jia, Facile synthesis of ZnS nanoparticles and their excellent photocatalytic performance, Ceramics International, 41, 2015, 6645-6652.

[4] A. Asfaram, M. Ghaedi, S. Hajati, M. Rezaeinejad, A. Goudarzi and M. K. Purkait, Rapid removal of Auramine-O and Methylene blue by ZnS: Cu nanoparticles loaded on activated carbon: A response surface methodology approach, Journal of the Taiwan Institute of Chemical Engineers, 2015,

[5] M. Arshad, M. M. Ansari, A. S. Ahmed, P. Tripathi, S. Ashraf, A. Naqvi and A. Azam, Band gap engineering and enhanced photoluminescence of Mg doped ZnO nanoparticles synthesized by wet chemical route, Journal of Luminescence, 161, 2015, 275-280.

[6] D. Chhikara, K. Srivatsa and S. K. Muthusamy, on the synthesis and characterization of ZnO/MgO nanocomposite by thermal evaporation technique, Solid State Sciences, 37, 2014, 108-113.

[7] H. R. Pouretedal, A. Norozi, M. H. Keshavarz and A. Semnani, Nanoparticles of zinc sulfide doped with manganese,

nickel and copper as nanophotocatalyst in the degradation of organic dyes, Journal of hazardous materials, 162, 2009, 674-681.

[8] K. Barick, M. Aslam and D. Bahadur, Fabrication and properties of Co doped ZnO spherical assemblies, Journal of Alloys and Compounds, 587, 2014, 282-286.

[9] M. Mittal, M. Sharma and O. Pandey, UV–Visible light induced photocatalytic studies of Cu doped ZnO nanoparticles prepared by co-precipitation method, Solar Energy, 110, 2014, 386-397.

[10] G. Murugadoss and M. R. Kumar, Synthesis and optical properties of monodispersed Ni2+-doped ZnS nanoparticles, Applied Nanoscience, 4, 2014, 67-75.

[11] E. Mohagheghpour, M. Rabiee, F. Moztarzadeh, M. Tahriri, M. Jafarbeglou, D. Bizari and H. Eslami, Controllable synthesis, characterization and optical properties of ZnS: Mn nanoparticles as a novel biosensor, Materials Science and Engineering: C, 29, 2009, 1842-1848.

[12] S. Li, Z. Wu, W. Li, Y. Liu, R. Zhuo, D. Yan, W. Jun and P. Yan, One-pot synthesis of ZnS hollow spheres via a low-temperature, template-free hydrothermal route, CrystEngComm, 15, 2013, 1571-1577.

[13] J. Sun, G. Chen, Y. Feng and Y. Wang, Ag/Cu co-doped ZnS–In 2 S 3 solid solutions: facile synthesis, theoretical calculations and enhanced photocatalytic activity, RSC Advances, 4, 2014, 44466-44471.

[14] Y. Liu, G. Xi, S. Chen, X. Zhang, Y. Zhu and Y. Qian, New ZnS/organic composite nanoribbons: characterization, thermal stability and photoluminescence, Nanotechnology, 18, 2007, 285605.

[15] X. Liu, X. Chen, X. Cui and R. Yu, The structure and multifunctional behaviors of Mn–ZnO/Mn–ZnS nanocomposites, Ceramics International, 40, 2014, 13847-13854.

[16] M. Ashokkumar and S. Muthukumaran, Effect of Ni doping on electrical, photoluminescence and magnetic behavior of Cu doped ZnO nanoparticles, Journal of Luminescence, 162, 2015, 97-103.

[17] U. Senapati, D. Jha and D. Sarkar, Green Synthesis and Characterization of ZnS nanoparticles, Res. J. Physical Sci, 1, 2013, 1-6.

[18] P. Bandyopadhyay, A. Dey, R. Basu, S. Das and P. Nandy, Synthesis and characterization of copper doped zinc oxide nanoparticles and its application in energy conversion, Current Applied Physics, 14, 2014, 1149-1155.

[19] D. M. A. Raj, A. D. Raj, A. A. Irudayaraj, R. Josephine, M. S. Kumar and M. Thambidurai, One step synthesis, optimization and growth mechanism carambola fruit shaped CuO nanostructures: electrochromic performance, Journal of Materials Science: Materials in Electronics, 26, 2015, 659-665.

[20] D. M. A. Raj, A. D. Raj and A. A. Irudayaraj, Facile synthesis of rice shaped CuO nanostructures for battery application, Journal of Materials Science: Materials in Electronics, 25, 2014, 1441-1445.

[21] D. C. Mayo, C. E. Marvinney, E. S. Bililign, J. R. McBride, R. R. Mu and R. F. Haglund, Surface-plasmon mediated photoluminescence from Ag-coated ZnO/MgO core–shell nanowires, Thin Solid Films, 553, 2014, 132-137.